

The Jaws of *Nereis*: Microstructure and Mechanical Properties

Henrik Birkedal^{1,4}, Chris Broomell², Rashda K. Khan¹, Nelle Slack³, Helga C. Lichtenegger^{1,5}, Frank Zok³, Galen D. Stucky^{1,3}, J. Herbert Waite^{1,2}

¹Department of Chemistry and Biochemistry, ²Department of Molecular, Cellular, and Developmental Biology, and ³Materials Department, University of California, Santa Barbara, CA 93106, U.S.A.

⁴ Present address: Department of Chemistry, University of Aarhus, 140 Langelandsgade, DK-8000 Aarhus, Denmark.

⁵ Present address: Department of Materials Science and Technology, Vienna University of Technology, Favoritenstrasse 9-11, A-1040 Wien, Austria.

ABSTRACT

The jaws of the marine worm *Nereis* sp. are made of protein fibers and are reinforced by zinc. Here we study a transverse section through the jaw using optical microscopy and nanoindentation. Optical microscopy images demonstrate a complex microstructure which includes channels that extend throughout the jaw. We suggest that these channels may be related to jaw remodeling. The mechanical results reveal spatial variations in both indentation hardness and reduced modulus. Specifically, the toothed side of the jaw (used for grasping food) is harder than the remainder of the jaw and the very exterior surface is hardest.

INTRODUCTION

Nature uses a host of strategies for the design of hard tissues such as teeth and jaws including biomineralization [1] but also protein cross-linking of cuticle [2]. We have previously shown that the related polychaete marine worms *Glycera* sp. and *Nereis* sp. use two different designs for their jaw systems: *Glycera* is partially mineralized [3] while *Nereis* is not [4]. *Glycera dibranchiata* presents the first instance of the use of a copper biomineral, namely atacamite ($\text{Cu}_2(\text{OH})_3\text{Cl}$) [3,5]. *Nereis* in contrast contains non-mineralized zinc [4,6,7,8]. The zinc is concentrated towards the jaw tip, the portion of the jaw that is exposed to the greatest mechanical stress. Indeed, we found a correlation between zinc content and both indentation hardness and modulus [4]. The *Nereis* jaws also contain the halogens Cl, Br and I [4, 7]. The chlorine concentration is linearly dependent on the Zn concentration suggesting that they occur together in the jaws. The zinc/chlorine is not bound in a detectable crystalline phase. However, the histidine concentration in the protein matrix also increases towards the jaw tip and on the basis of EXAFS data we suggested that a $\text{Zn}(\text{His})_3\text{Cl}$ binding motif is a fair representation of the average zinc environment [4]. The heavier halogens, Br and I, are concentrated in the surface region of the jaw [7,9]. Herein we report a study of a transverse cross-section of a *Nereis* jaw by optical microscopy and nanoindentation and show that the toothed side of the jaw, in particular its surface, is the hardest.

EXPERIMENTAL DETAILS

Jaws were dissected from recently thawed *Nereis virens* specimens (Maine Bait Company, ME, USA) that had been put to death by rapid freezing at -80°C . The jaws were washed three times in 2.4 M guanidine-HCl/5% acetic acid and five times in distilled water, followed by drying in air.

For nanoindentation, the jaws were embedded in EpoFix (Electron Microscopy Sciences, PA, USA). Flat surfaces suitable for testing were obtained by cutting the embedded specimen with a Leica ultramicrotome using a Diatome diamond knife (Electron Microscopy Sciences, Hatfield, PA, USA). The samples were imaged using optical microscopy before, Figure 1, and after indentation. Herein we discuss a transverse cross section made roughly 15% below the jaw tip. Nanoindentation measurements were carried out with a Hysitron TriboIndenter (Hysitron, MN, USA). The indents were made with a cube corner diamond indenter with a tip radius of 40–60 nm (Hysitron, MN, USA). Several test indents were made to assess which indentation parameters gave the best results. The final measurements used the following program: load from 0 to 500 μN in 5 s, hold for 60 s to relax viscoelastic effects, unload to 0 μN in 5 s. Regions of the jaw just around the indents were imaged before and after indentation using the diamond tip. These images revealed that the indent area was triangular with sides of about 1.1 μm . Several lines of indents were made as well as a grid of indents over a $200 \times 100 \mu\text{m}$ area. The indents were spaced at least 10 μm apart to eliminate any potential interactions between stress fields of neighboring indents. The indentation hardness, H , and reduced modulus, E_r , were extracted following the method developed by Oliver and Pharr [10]. Since the Poisson ratio of the jaw is unknown, we report only the reduced modulus, rather than the Young's modulus itself.



Figure 1. Composite optical micrograph of a transverse cross-section of a *Nereis* jaw obtained using a microtome. The inset shows a picture of a worm with everted proboscis as well as a whole extracted jaw (composite). The whole worm is viewed onto the ventral side.

DISCUSSION

The *Nereis* jaws are about 5 mm long. They are asymmetrical and have a complicated curvature as illustrated in the insets of Figure 1. The jaws have a toothed side, which is the side engaged in contact with foreign matter when the jaws are used to grasp food. Perpendicular to this direction, along the transverse cross section, there is a distinctly straight surface, indicated in Figure 1, opposite to a bulgy side. The jaw cross-section is optically quite inhomogeneous, Figure 1, with large variations in contrast. We suggest that these reflect variations in the jaw mesostructure, possibly variations in orientation of the protein fibrils from which the jaw is made [4]. The round holes in the jaw center are channels that extend to the jaw tip. They are about 5–25 μm in diameter. The role of these channels is unclear, but they could provide cellular access for jaw remodeling. It is known that the jaws grow throughout the life-cycle of the worms [11], but the details of jaw growth remain unclear.

The results of the nanoindentation experiments are given in Figure 2. Average values of H and E_r are given in Table I. There are large spatial variations in jaw hardness and reduced

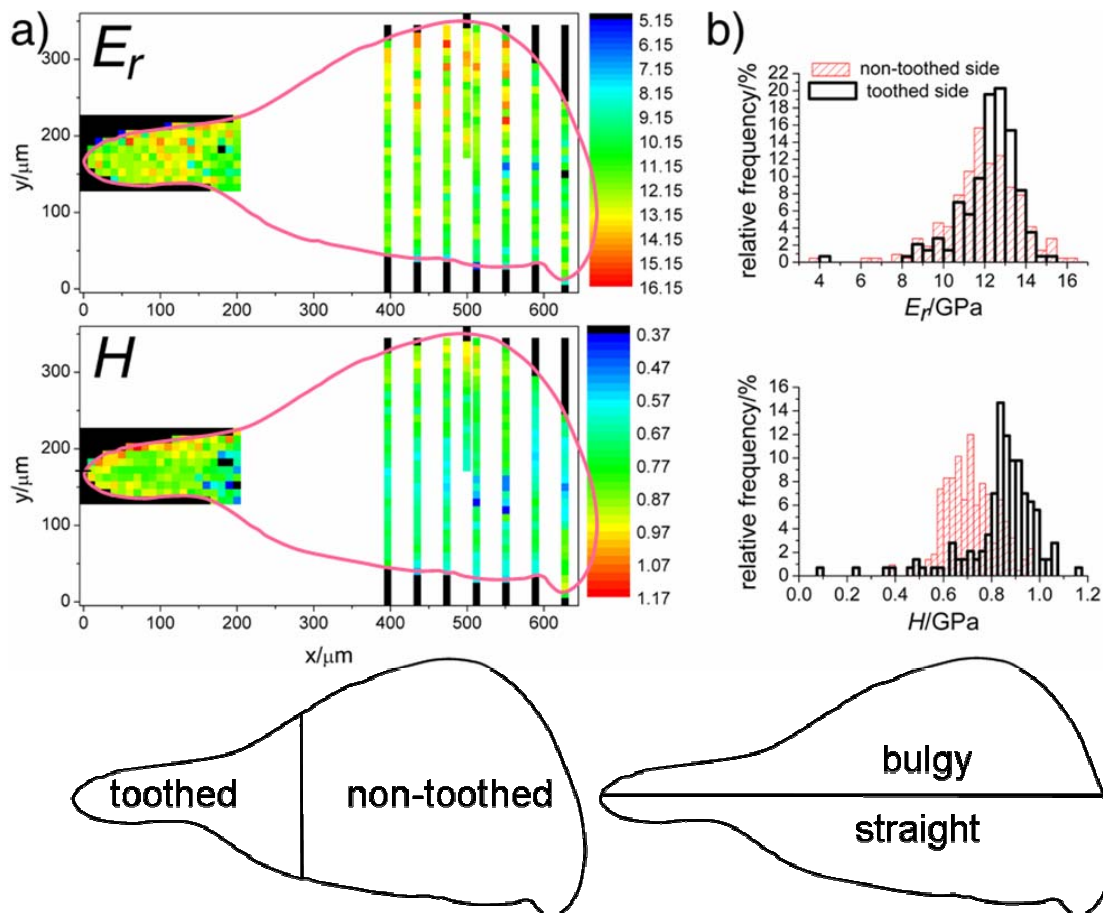


Figure 2. Results of nanoindentation on the jaw cross-section shown in Figure 1. Both the reduced modulus, E_r , and the indentation hardness, H , are given in GPa. a) Position resolved plots of E_r (top) and H (bottom). The jaw outline is marked in pink. b) histograms of E_r (top) and H (bottom) for the toothed side ($x < 300$ mm) and the non-toothed side of the indent datasets shown in a). The two sketches in the bottom part of the figure delineate the division of the jaw into specific areas.

Table I. Average values of indentation hardness, H , and reduced modulus, E_r , in the jaw cross-section shown in Figure 2. For each entry we give the number of indents (Indents), the average value (value), the standard deviation of the mean (SD) and the standard error (SEM).

Region	Indents	H (GPa)			E_r (GPa)		
		value	SD	SEM	value	SD	SEM
Jaw, all data	360	0.765	0.142	0.007	12.06	1.62	0.09
toothed side	143	0.842	0.153	0.013	12.23	1.43	0.12
non-toothed side	217	0.715	0.108	0.007	11.95	1.72	0.12
straight side	160	0.724	0.133	0.011	11.40	1.58	0.12
bulgy side	200	0.799	0.139	0.010	12.59	1.45	0.10

modulus throughout the transverse section as can be seen from the standard deviation of the distributions given in Table I. It is apparent from Figure 2a that there are systematic spatial variations in the mechanical characteristics of the jaw – especially the hardness. Specifically, the jaw is harder on the toothed side than elsewhere. To quantify this, we divided the nanoindentation data into two sets: one corresponding to the toothed side ($x < 300$ mm in Figure 2a) and the second to the remainder, see the bottom inset in Figure 2. Figure 2b presents the resulting histograms of E_r and H . The H distribution is sharper and centered at higher hardness values in the toothed region. The average hardness is significantly higher in the toothed part than in the non-toothed part based on the Student's t -test ($P < 10^{-4}$). The difference in modulus was insignificant (Student's t -test, $P > 0.1$). The toothed side of the jaw is the one that is in contact with foreign material when the jaws are used for grasping. Thus this part of the jaw needs to be particularly hard to ensure a reasonable wear resistance. Bryan and Gibbs showed that the toothed half of the jaw contains higher concentrations of Zn and Fe than the non-toothed side [7]. They found a zinc-content of 2.22 wt% in the toothed half versus 1.40 wt% in the remaining half. The iron content is much smaller, 0.070 and 0.027 wt% for the toothed and non-toothed half, respectively. They found manganese in roughly the same amounts as Fe, but the distribution between toothed and non-toothed half was opposite. This zinc asymmetry, combined with our observations of a linear correlation between zinc content and both hardness and modulus along the long axis of the jaw [4], indicates that the animal at least in part uses zinc to adjust the local mechanical properties. It was found in a previous study that hardness and stiffness decreased over the length of the jaw (from tip to base) in parallel with the zinc and His levels [13], thus suggesting local hardening by coordination of His and zinc. Here we show that hardness gradients are also found perpendicular to the longitudinal axis. The decrease of the hardness from the toothed to the non-toothed side corresponds to a similar decrease in His levels as reported in [3].

There is also an asymmetry between the straight and bulgy side. To demonstrate this asymmetry, we divide the jaw at the midpoint of tooth (Figure 2) such that the straight side comprises all indents with $y < 170$ μm . The bulgy side is both stiffer (~9%) and harder (~5%) than the straight side (Student's t -test, $P < 10^{-4}$). The observation that the bulgy side is stiffer and harder than the straight one could be related to the recent observation that the pharynx is everted during burrowing [13]. This motion allows the worm to move by propagating cracks in the sandy medium in which it lives. For this purpose, the side of the jaw engaged in propagating cracks

should be hard and stiff. Further studies of the relation between local jaw mechanical properties and actual jaw use by the animal will be most interesting.

CONCLUSIONS

In conclusion, we have shown that the transverse section of the *Nereis* jaw is quite inhomogeneous. The inhomogeneities seen in optical microscopy may be indicative of the different mesostructures of the jaw. We have also discovered channels which run along the length of the jaw which may be critical for jaw growth and remodeling. Our nanoindentation investigations show that *Nereis* jaw exhibits property gradients both along its length (from tip to base) and perpendicular to the jaw axis. Moreover, there is a pronounced asymmetry in the transverse direction: the toothed side being harder than the remainder of the jaw and the bulgy side being stiffer. The variation in mechanical properties, especially hardness, may also correlate with the mesostructure visible by optical microscopy.

The property gradients along the jaw axis are possibly related to a need for the hard outside world to interact with the soft worm tissue via the jaws without building up large stresses [14]. The region of highest hardness is the outer rim of the toothed side, in particular on the bulgy side. Such a thick hard coating could lead to good abrasion resistance without introducing brittleness [12], a key requirement for the jaws. Finally, the animals have only restricted access to metals such as zinc. Meticulously measuring out the metal in just sufficient quantities may allow the worms to obtain the needed mechanical properties without paying an excessive metal-acquisition penalty.

ACKNOWLEDGEMENTS

We thank the participants in the Thursday biomaterials meetings at UCSB, in particular members of the Stucky, Waite, Morse and Hansma groups, for helpful discussions. We gratefully acknowledge financial support from the NIH under contract DE014672. HCL thanks the Fonds zur Förderung der Wissenschaftlichen Forschung (Austria) for additional funding (Awards J2184 and T190). HB thanks the Danish Natural Sciences Research Council for additional funding and the Danish Natural Sciences Research Council and the Danish Technical Research Council for a Steno research assistant professor fellowship that funded the final stages of this project. This work made use of MRL Central Facilities supported by the MRSEC Program of the National Science Foundation under award No. DMR00-80034.

REFERENCES

1. H.A. Lowenstam and S. Weiner, *On Biomineralization* (Oxford University Press, New York, NY, 1989).
2. S.O. Andersen, M.G. Peter and P. Roepstorff, *Comp. Biochem. Physiol. B* **113**, 689 (1996).
3. H.C. Lichtenegger, T. Schöberl, M.H. Bartl, H. Waite and G.D. Stucky, *Science* **298**, 389 (2002).
4. H.C. Lichtenegger, T. Schöberl, J.T. Ruokolainen, J.O. Cross, S.M. Heald, H. Birkedal, J.H. Waite and G.D. Stucky, *Proc. Natl. Acad. U.S.A.* **100**, 9144 (2003).
5. H.C. Lichtenegger, H. Birkedal, D.M. Casa, J.O. Cross, S.M. Heald, J.H. Waite and G.D. Stucky, *Chem. Mater.* In press (2005).

6. G.W. Bryan and P.E. Gibbs, *J. Mar. Biol. Ass. U.K.* **59**, 969 (1980).
7. G.W. Bryan and P.E. Gibbs, *J. Mar. Biol. Ass. U.K.* **60**, 641 (1980).
8. M. Eriksson and M. Elfman, *Lethaia* **33**, 75 (2000).
9. H. Birkedal, R.K. Khan, N. Slack, C. Broomel, H.C. Lichtenegger, F. Zok, G.D. Stucky and J.H. Waite, *in preparation* (2005).
10. W.C. Oliver and G.M. Pharr, *J. Mater. Res.* **7**, 1564 (1992).
11. P.J. Olive in *Skeletal Growth of Aquatic Organisms: Biological Records of Environmental Change* edited by D.C. Rhoads and R.A. Lutz (Plenum Press, New York, NY, 1980) pp. 561-592.
12. S. Suresh, *Science* **292**, 2447 (2001).
13. K.M. Dorgan, P.A. Jumars, B. Johnson, B.P. Boudreau and E. Landis, *Nature* **433**, 45 (2005).
14. J.H. Waite, H.C. Lichtenegger, G.D. Stucky and P. Hansma, *Biochemistry* **43**, 7653 (2004).